

Spin and charge dynamics of the 2D t - J model at intermediate electron densities: absence of spin-charge separation

R. Eder and Y. Ohta

Department of Applied Physics, Nagoya University, Nagoya 464-01, Japan

We present an exact diagonalization study of the dynamical spin and density correlation functions in small clusters of $t - J$ model, focussing on the regime of intermediate and low electron densities, $\rho_e < 0.5$. In 2D both correlation functions agree remarkably well with the convolution of the single-particle spectral function, i.e. the simplest estimate possible within a Fermi liquid picture. Deviations from the convolution are shown to originate from symmetry-related selection rules, which are unaccounted for in the convolution estimate. For all fillings under consideration, we show that the low energy peaks originate from particle-hole excitations between the Fermi momenta, as expected for a Fermi liquid. We contrast this with the behaviour in 1D, where spin and density correlation function show the differences characteristic of spin-charge separation and where neither correlation function is approximated well by the convolution.

74.20.-Z, 75.10.Jm, 75.50.Ee

A much discussed issue in the theory of high-temperature superconductivity is the question whether strongly correlated electron models in 2D share the most striking feature of their 1D counterparts, spin charge separation. Whereas in a Fermi liquid the low lying spin and density excitations can be modelled by particle-hole (i.e. composite) excitations of the fermionic quasiparticles, which represent the ‘most elementary’ excitations of the system, the situation is reversed in a spin-charge separated system. There, the soliton-like spin and density excitations are themselves the elementary excitations, and the physical electrons can be considered as composite excitations.

By numerical diagonalization one can obtain the exact excitation spectra of small clusters and should thus, at least in principle, be able to decide whether they are consistent with any given theoretical scenario. We therefore have performed a study of the dynamical spin and density correlation functions of the t - J model, which reads

$$H = -t \sum_{\langle i,j \rangle, \sigma} (\hat{c}_{i,\sigma}^\dagger \hat{c}_{j,\sigma} + H.c.) + J \sum_{\langle i,j \rangle} [\mathbf{S}_i \cdot \mathbf{S}_j - \frac{n_i n_j}{4}].$$

The \mathbf{S}_i are the electronic spin operators, $\hat{c}_{i,\sigma}^\dagger = c_{i,\sigma}^\dagger (1 - n_{i,-\sigma})$ and the sum over $\langle i,j \rangle$ stands for a summation over all pairs of nearest neighbors. All results to be presented below have been obtained for 1D and 2D 16 site clusters, with the parameter value $J/t=0.4$. In the present study we restrict ourselves to intermediate and low electron densities, where the results are more easily understood than near half-filling [1]. To be more precise, in this doping regime the excitation spectrum of the 2D t - J model turns out to be completely consistent with the Fermi-liquid derived particle-hole picture, even deviations from the noninteracting case are small.

Our results suggest that throughout the range of dopings studied, the t - J model represents a not even very strongly correlated Fermi liquid. No detail of our results would necessitate the introduction of the concept of spin charge separation.

Using the standard Lanczos algorithm we computed the dynamical spin (SCF) and density (DCF) correlation functions:

$$C_\alpha(\mathbf{q}, \omega) = \frac{1}{\pi} \Im \langle \Psi_0 | O_\alpha^\dagger \frac{1}{\omega - (H - E_0) - i0^+} O_\alpha | \Psi_0 \rangle.$$

Here $|\Psi_0\rangle$ (E_0) denotes the ground state wave function (ground state energy), and as the operator O we choose the Fourier transform of either the density operator $n_{i,\uparrow} + n_{i,\downarrow}$ ($\alpha = d$) or the spin operator $(1 - \rho_e)(n_{i,\uparrow} - n_{i,\downarrow})$ ($\alpha = s$). We introduced an extra prefactor of $2(1 - \rho_e)$ for the z -spin operator because with this definition both correlation functions obey the same sum-rule,

$$\sum_{\mathbf{q} \neq 0} \int_0^\infty d\omega C_\alpha(\mathbf{q}, \omega) = \rho_e (1 - \rho_e),$$

which facilitates their comparison. In a system of noninteracting particles, the above two particle Green’s functions can be expressed as the convolution of the single particle photoemission (PES) and inverse photoemission (IPES) spectrum, i.e.

$$C_c(\mathbf{q}, \omega) = \frac{2}{N^2} \sum_{\mathbf{k}} \int d\omega' A_{PES}(\mathbf{k}, \omega') A_{IPES}(\mathbf{q} - \mathbf{k}, \omega - \omega').$$

Having computed the PES and IPES spectra by the Lanczos method we can replace the δ -peaks in these functions by Lorentzians and obtain the convolution numerically. Thereby the broadening of the δ -peaks in the spectral function was taken 1/2 of the one for the correlation functions, because the numerical convolution effectively

doubles the width of the peaks. The convolution obeys the sum rule

$$\sum_{\mathbf{q} \neq 0} \int_0^\infty d\omega C_c(\mathbf{q}, \omega) = \rho_e(1 - \rho_e) - \frac{2}{N^2} \sum_{\mathbf{k}} n_{\mathbf{k}}(m(\delta) - n_{\mathbf{k}}),$$

where $n(\mathbf{k}) = \langle \hat{c}_{\mathbf{k},\sigma}^\dagger \hat{c}_{\mathbf{k},\sigma} \rangle$ denotes the ground state momentum distribution and $m(\delta) = (1 + \delta)/2$ with δ the hole concentration. The last term is different from 0 but turns out to be quite small, so that all spectral functions under consideration have a comparable integrated weight.

Approximating the spin and density correlation function by a mere convolution is a drastic approximation, which neglects for example all vertex corrections; as we will show now, for the electron densities under consideration it is nevertheless a remarkably good approximation. Figs. 1-4 compare the convolution estimate with the exact SCF and DCF for electron densities between 10/16 and 4/16. While the agreement for 6 holes is not yet very impressive (particularly for the SCF), the agreement becomes better and better with decreasing electron density. With the exception of the low energy peak structure at $(\pi, 0)$ and $(\pi/2, \pi/2)$ (which is determined by symmetry-related selection rules unaccounted for in the convolution, see below) the overall shape of the exact correlation functions is reproduced quite well, sometimes to the degree of a one-to-one correspondence between the dominant features. While SCF and DCF are not obviously identical, they both can be viewed as being derived by slight but different modifications of the convolution.

We now turn to the low energy peaks at $(\pi, 0)$ and $(\pi/2, \pi/2)$, indicated by arrows in Figs. 2-4. Obviously these are not reproduced well by the convolution. We will show that this is the consequence of point group selection rules, which are not accounted for in the convolution. Assuming the existence of a free electron like Fermi surface, the 6 hole ground state would correspond to a closed-shell configuration, where the momenta $(0, 0)$, $(\pm\pi/2, 0)$ and $(0, \pm\pi/2)$ are occupied. The ground states with lower electron densities then would have ‘holes’ in the outer shell of momenta, which are therefore only partially occupied. This is confirmed by the spectral function at $(\pi/2, 0)$, which shows only a PES peak immediately below the Fermi energy for 10 electrons, but both a PES peak immediately below and an IPES peak immediately above the Fermi energy for 8, 6 and 4 electrons. The low energy peaks in the convolution for momentum transfer $(\pi, 0)$ and $(\pi/2, \pi/2)$ then originate precisely from transitions within this shell of partially occupied momenta $(\pm\pi/2, 0)$, $(0, \pm\pi/2)$, as indicated in Fig. 4a. We adopt the hypothesis that the lowest states of the system can be described by a ‘cluster version’ of Fermi liquid theory. To be more precise, we assume that e.g. for the 8 electron case there is a one-to-one mapping of e.g. the lowest states of the cluster and ‘quasiparticle states’ of the type $a_{\mathbf{k},\uparrow} a_{\mathbf{k}',\downarrow} |FS\rangle$, where $a_{\mathbf{k},\sigma}$ annihilates a quasiparticle, $|FS\rangle$ denotes the closed shell Fermi sea of 10 non-

interacting electrons and \mathbf{k} and \mathbf{k}' are restricted to the shell of momenta $(\pm\pi/2, 0)$, $(0, \pm\pi/2)$. We next assume that there is a residual interaction between the quasiparticles, which lifts the degeneracy between the various states of this type with given total momentum. To simplify the notation we label the momenta as indicated in Fig. 4b. Then, from the fact that the exact 8 electron ground state is a spin singlet and has $d_{x^2-y^2}$ symmetry, we conclude that it should be modelled by the state

$$\frac{1}{2}(a_{1,\uparrow} a_{3,\downarrow} - a_{1,\downarrow} a_{3,\uparrow} - a_{2,\uparrow} a_{4,\downarrow} + a_{2,\downarrow} a_{4,\uparrow}) |FS\rangle. \quad (1)$$

This would also be consistent with the pronounced $d_{x^2-y^2}$ pairing correlations found for larger values of J/t at this electron density [2,3]. Next, the only states in our subspace with momentum $(\pi/2, \pi/2)$ are

$$\frac{1}{\sqrt{2}}(a_{3,\uparrow} a_{4,\downarrow} \pm a_{3,\downarrow} a_{4,\uparrow}) |FS\rangle. \quad (2)$$

The antisymmetric combination is a spin singlet and even under reflection by the $(1, 1)$ direction, so that its point group symmetry is incompatible with that of the ground state: there can be no peak in the DCF. The symmetric combination is a spin triplet and has an acceptable point group symmetry so that we expect a peak in the SCF. Both predictions are consistent with the exact spectra. The only possible state with momentum $(\pi, 0)$ and the required point group symmetry (even under reflections by both x and y axis) in the model space is

$$\frac{1}{\sqrt{2}}(a_{1,\uparrow} a_{1,\downarrow} + a_{3,\uparrow} a_{3,\downarrow}) |FS\rangle. \quad (3)$$

This is a spin singlet so that the SCF cannot have a low energy peak. Since the point-group symmetry of this state is consistent with the selection rules, we expect a low-energy peak in the DCF. Again both predictions are consistent with the exact spectra, although the weight of the low energy peak in the DCF is extremely small.

Next, literally the same explanation holds for the case of 4 electrons, if we replace the annihilation operators by creation operators, choose the fully occupied Γ -point as the ‘Fermi sea’ and replace $(3, 4) \rightarrow (1, 2)$ in (2). This is because like the 8 electron ground state, the 4 electron ground state is a spin singlet with $d_{x^2-y^2}$ symmetry. We thus expect a low energy peak in the DCF at $(\pi, 0)$ and in the SCF at $(\pi/2, \pi/2)$; inspection of the exact spectra shows, that this is indeed realized.

We turn to the case of 6 electrons. Here we have to use quasiparticle states with 4 holes in the 10-electron closed shell. The exact ground state has unusual quantum numbers: its total spin is $S = 2$ and it belongs to the B_2 (or d_{xy}) representation of the C_{4v} point group. This suggests to model the $S_z = -2$ member of the ground state multiplet by the state $a_{1,\uparrow} a_{2,\uparrow} a_{3,\uparrow} a_{4,\uparrow} |FS\rangle$, which obviously has the correct point group symmetry. The $S_z = 0$ member of the ground state multiplet (which we

are considering) can now in principle be obtained by acting twice with the spin raising operator. It is easy to see, however, that all necessary conclusions can already be drawn from the final states: introducing the operator $t_{i,j} = 1/\sqrt{2}(a_{i,\uparrow}a_{j,\downarrow} + a_{i,\downarrow}a_{j,\uparrow})$, which creates a spin triplet on the momenta i and j , the only state with total momentum $(\pi, 0)$ and the required point group symmetry (odd under reflection by both x - and y -axis) reads

$$\frac{1}{\sqrt{2}}(a_{1,\uparrow}a_{1,\downarrow} - a_{3,\uparrow}a_{3,\downarrow})t_{2,4}|FS\rangle. \quad (4)$$

This is a spin triplet, so that we expect a peak in the SCF but not in the DCF. Similarly, the state with maximal spin and momentum $(\pi/2, \pi/2)$ that is even under reflection by the $(1, 1)$ direction reads

$$\frac{1}{\sqrt{2}}(a_{3,\uparrow}a_{3,\downarrow}t_{1,4} + a_{4,\uparrow}a_{4,\downarrow}t_{2,3})|FS\rangle. \quad (5)$$

Again, this is a triplet, so that we expect a peak in the SCF but not in the DCF. All predictions are consistent with the numerical spectra.

We thus have shown that the low energy peak structure can be understood completely by a simple ‘cluster Fermi liquid theory’, which relies on nothing more than elementary selection rules. To further strengthen the evidence for this interpretation, we now compare the electron momentum distribution $n(\mathbf{k}) = \langle c_{\mathbf{k},\sigma}^\dagger c_{\mathbf{k},\sigma} \rangle$ in the ground state (GS) to that of the final states (FS) associated with the low-energy peaks in the SCF and DCF, i.e. we consider

$$\Delta n(\mathbf{k}) = n_{FS}(\mathbf{k}) - n_{GS}(\mathbf{k}). \quad (6)$$

Based on the above ‘model wave functions’, we can predict the changes of the quasiparticle occupation numbers which accompany the respective spin or density excitation. These are listed in Table I. Up to a constant factor due to the wave function renormalization constant Z , the exact $\Delta n(\mathbf{k})$ then should be the same.

To obtain the final state wave functions, we take advantage of the fact that the energies of the low energy peaks give highly precise estimates for the eigenenergies E_{final} of the SCF or DCF final states. Thus, by applying powers of $(H - E_{final})^{-1}$ to some randomly chosen trial state (thereby employing the conjugate gradient algorithm) we can efficiently converge out the respective final state wave function [4] and obtain its momentum distribution. Then, Figs. 7-9 show the $\Delta n(\mathbf{k})$ for all low lying peaks in both SCF and DCF. By comparison with Table I it can be seen that the exact results are indeed completely consistent with the particle-hole picture: the changes are always substantially larger for the Fermi momenta than for any other momentum, the reduction of the magnitude of $\Delta n(\mathbf{k})$ as compared to the ‘free electron’ estimate suggests values of the quasiparticle weight Z between 0.6 (for 8 electrons) and 0.8 (for 4 electrons). The losses of $n(\mathbf{k})$ at the Fermi momenta always exceed

the gains; this is probably due to an enhanced scattering in the final (=excited) states. We thus have rather unambiguous evidence for the validity of the Fermi liquid like particle-hole picture at low frequencies. For higher frequency the good agreement between the exact correlation functions and the convolution strongly suggests the same.

We now turn to a comparison with the 1D model, where spin charge separation rather than Fermi liquid behaviour is known to be realized at all doping levels [5]. Fig. 5 compares the SCF and DCF with the convolution of the single particle spectral function for $\rho_e=0.5$. The Fermi momentum is $k_F=\pi/4$, and SCF and DCF show their lowest energy excitation at different momenta, $2k_F=\pi/2$ and $4k_F=\pi$, respectively, which is characteristic of spin charge separation [5]. Unlike in 2D neither correlation function is approximated well by the convolution. The latter consists almost entirely of structureless continua, without the sharp peaks of the exact correlation functions.

For the low density regime our results are consistent with those of Jagla *et al.* [6]. These authors studied the group velocity of spin and charge excitations in small clusters and found different velocities for spin and charge in 1D (indicating spin charge separation) but identical velocities (indicating absence of spin charge separation) in 2D. On the other hand, evidence for spin charge separation at electron densities 0.75 and 0.2 was seen by Putikka *et al.* [7] in the static SCF and DCF of the 2D $t-J$ model obtained by high-temperature expansion. However, a subsequent cluster study of the same quantities by Chen *et al.* [8] could not strengthen this evidence: the DCF showed no indication of a singularity at the ‘characteristic wavevector’ for spinless Fermions. Moreover the *dynamical* SCF and DCF differ drastically for low and high doping [1] so that it seems not very plausible that they both can be described by the same physics. Our results show that while for low electron density the peak structure of SCF and DCF is similar and consistent with the convolution, there are differences in the pole strengths. Thus, while SCF and DCF apparently can be explained by particle-hole transitions between analogous states, the matrix elements are different. This would support an explanation of the the static correlation functions e.g. by RPA calculations for the large- U Hubbard Model [9].

In summary, we have studied the spin and density correlation function for intermediate and low electron densities in the $t-J$ model. For a spin-charge separated system, (i.e. in 1D), these two correlation functions cannot adequately be described in a particle-hole excitation picture. Contrary to this, our results for 2D show that the simplest estimate based on the particle-hole excitation picture, namely the convolution of the single particle spectral function, provides a remarkably good description of these correlation functions. The low energy peak structure can be completely explained by a simple ‘cluster Fermi liquid theory’ which relies only on the particle-

hole picture and elementary selection rules. The respective particle-hole transitions can be directly made visible in the momentum distribution. Our exact results thus suggest that for the less than quarter filled case the t - J model has a fairly conventional particle-hole type excitation spectrum, and represents a not even very strongly correlated Fermi liquid. There is no need to invoke spin-charge separation to understand the dynamics of the $2D$ t - J model for the electron densities under consideration. It is interesting to note that for electron densities near half-filling (i.e. 2 and 4 holes in the 4×4 cluster) the situation changes completely: the DCF consists almost entirely of incoherent, high-energy continua, the SCF has sharp low energy peaks and almost no continua [1]. The dominant spin excitation at (π, π) is a spin-wave like collective mode, i.e. a remnant of the undoped system; only spin excitations with different momentum transfer still correspond to particle-hole transitions [10]. In fact, quite a number of physical quantities show a significant change at hole concentration ~ 0.2 - 0.3 : the doping dependence of the Drude weight [11], the temperature dependence of the susceptibility [12], the sign of the Hall constant [13]. For $J=0$ Chiappe *et al.* [14] have shown that the overlap of the exact cluster ground state with Gutzwiller wave functions drops sharply from ~ 1 for low and intermediate electron densities to ~ 0 for high density. The clear distinction which can be seen in a wide variety of physical quantities suggests to assume two quite different phases for the $2D$ t - J model as a function of doping: for $\rho_e < 0.7$ - 0.8 there seems to be a fairly conventional Fermi liquid, with a ground state that is ‘adiabatically connected’ to the noninteracting one and correlations are of little importance. Near half-filling, the correlations dominate and the system seems to be continuous with the insulator: the spectral function shows rigid-band behaviour [15] with increasing doping, the Fermi surface takes the form of hole pockets [16,17], the spin excitation spectrum is reminiscent of the undoped Heisenberg anti-ferromagnet [10].

It is a pleasure to acknowledge numerous instructive discussions with Professor S. Maekawa and Dr. T. Tohyama. Financial support of R.E. by the Japan Society for the Promotion of Science is most gratefully acknowledged. Parts of the computations were carried out at the Institute for Molecular Science, Okazaki.

FIG. 1. Spin correlation function (right column, dotted line) and density correlation function (left column, dotted line) as compared to the convolution of the single particle spectral function (full line). All spectra are for the 4×4 cluster t - J model with 10 electrons and $J/t = 0.4$.

FIG. 2. Same as Fig. 1 for 8 electrons.

FIG. 3. Same as Fig. 1 for 6 electrons.

FIG. 4. Same as Fig. 1 for 4 electrons.

FIG. 5. Possible particle-hole transitions between the ‘Fermi momenta’ in the 4×4 cluster (a), labelling of the ‘Fermi momenta’ (b).

FIG. 6. Difference of $n(\mathbf{k})$ for the final states belonging to the low energy peaks indicated by arrows in Fig. 2 and $n(\mathbf{k})$ for the ground state i.e. the quantity $\Delta n(\mathbf{k})$ defined in (6). The figure shows all momenta in the Brillouin zone, the ‘Fermi momenta’ of Fig. 5 are indicated by dark symbols, the top right corner corresponds to (π, π) . The number of electrons is 8.

FIG. 7. Same as Fig. 6 for 6 electrons.

FIG. 8. Same as Fig. 6 for 4 electrons.

FIG. 9. a: Comparison of convolution (full line) and exact DCF (dotted line) for the $1D$ 16-site chain with 8 electrons and $J/t = 0.4$. b: same as (a) but for the SCF.

TABLE I. Change of the electron occupation numbers of the Fermi momenta as obtained from the model wave functions for the SCF and DCF final states.

N_e	\mathbf{k}	α	$(\frac{\pi}{2}, 0)$	$(0, \frac{\pi}{2})$	$(-\frac{\pi}{2}, 0)$	$(0, -\frac{\pi}{2})$
8	$(\pi, 0)$	DCF	-0.25	+0.25	-0.25	+0.25
8	$(\frac{\pi}{2}, \frac{\pi}{2})$	SCF	+0.25	+0.25	-0.25	-0.25
6	$(\pi, 0)$	SCF	0.00	0.00	0.00	0.00
6	$(\frac{\pi}{2}, \frac{\pi}{2})$	SCF	+0.25	+0.25	-0.25	-0.25
4	$(\pi, 0)$	DCF	+0.25	-0.25	+0.25	-0.25
4	$(\frac{\pi}{2}, \frac{\pi}{2})$	SCF	+0.25	+0.25	-0.25	-0.25

-
- [1] T. Tohyama, P. Horsch, and S. Maekawa, unpublished.
 - [2] E. Dagotto and J. Riera, Phys. Rev. Lett. **70**, 682 (1993).
 - [3] Y. Ohta *et al.*, Phys. Rev. Lett. **73**, 324 (1994).
 - [4] This is known as the inverse iteration algorithm; see e.g. A. Jennings, Matrix Computation for Engineers and Scientists, John Wiley & Sons, Chichester New York Brisbane Toronto (1977).
 - [5] P. A. Bares and G. Blattter, Phys. Rev. Lett. **64**, 2567 (1990).
 - [6] E. A. Jagla, K. Hallberg, and C. A. Balseiro, Phys. Rev. B **47**, 5849 (1993).
 - [7] W. O. Putikka *et al.*, Phys. Rev. Lett. **73**, 170 (1994).
 - [8] Y. C. Chen *et al.* Phys. Rev. B **50**, 655 (1994).
 - [9] N. Bulut *et al.*, Phys. Rev. B **47**, 2742 (1993).
 - [10] R. Eder and Y. Ohta, unpublished (SISSA-preprint cond-mat 9408057).
 - [11] E. Dagotto *et al.*, Phys. Rev. B **45**, 10741 (1992).
 - [12] T. Tohyama *et al.* Physica C **215**, 382 (1993).
 - [13] H. E. Castillo and C. A. Balseiro, Phys. Rev. Lett. **68**, 121 (1992).
 - [14] G. Chiappe *et al.* Phys. Rev. B **48**, 16539 (1993).
 - [15] R. Eder, Y. Ohta, and T. Shimoizato, Phys. Rev. B **50**, 3350 (1994).
 - [16] A. Moreo and D. Duffy,
(SISSA-preprint cond-mat 9407039).
 - [17] R. Eder and Y. Ohta, unpublished (SISSA-preprint cond-mat 9407097)

Fig. 1

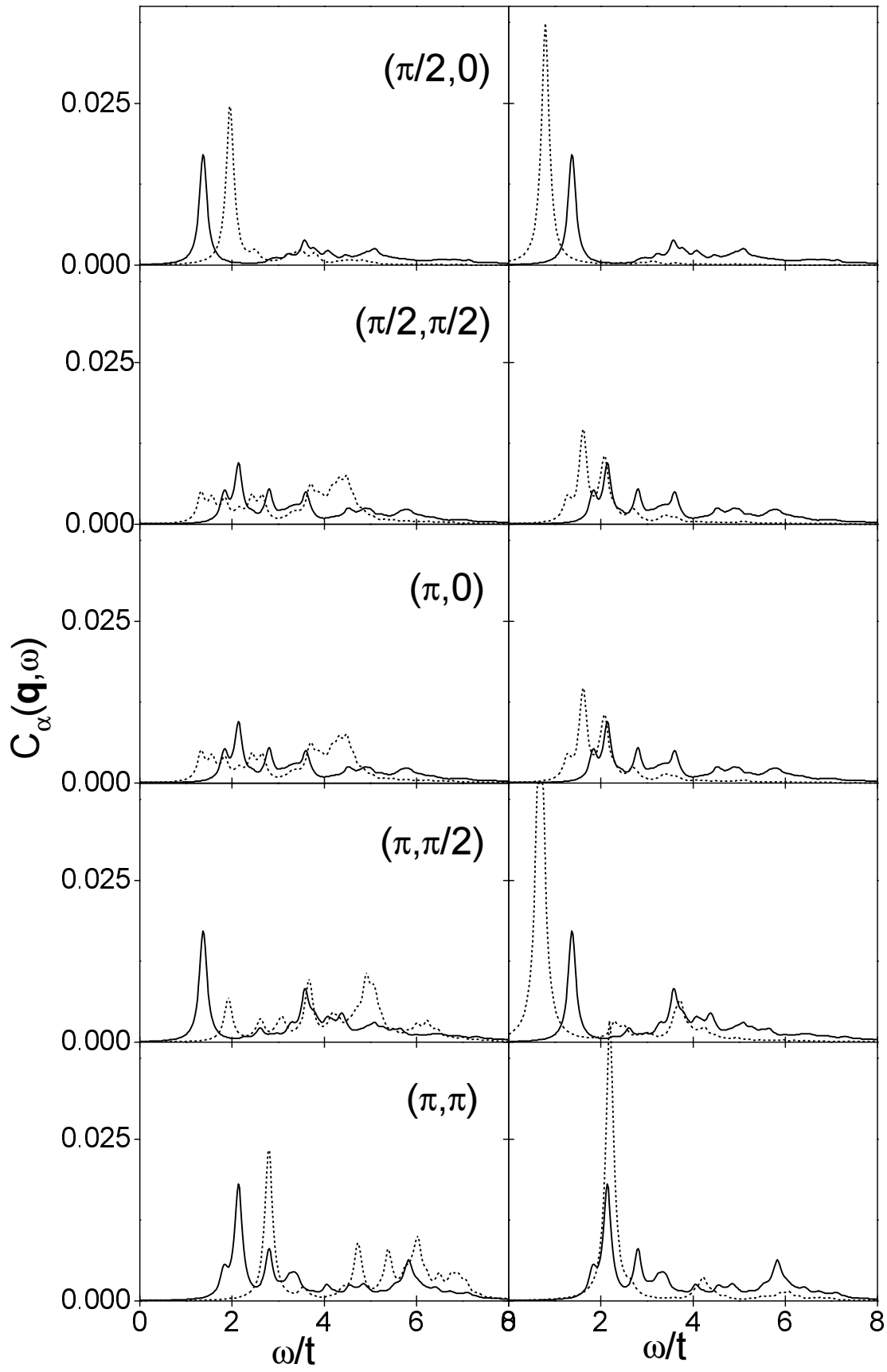


Fig. 2

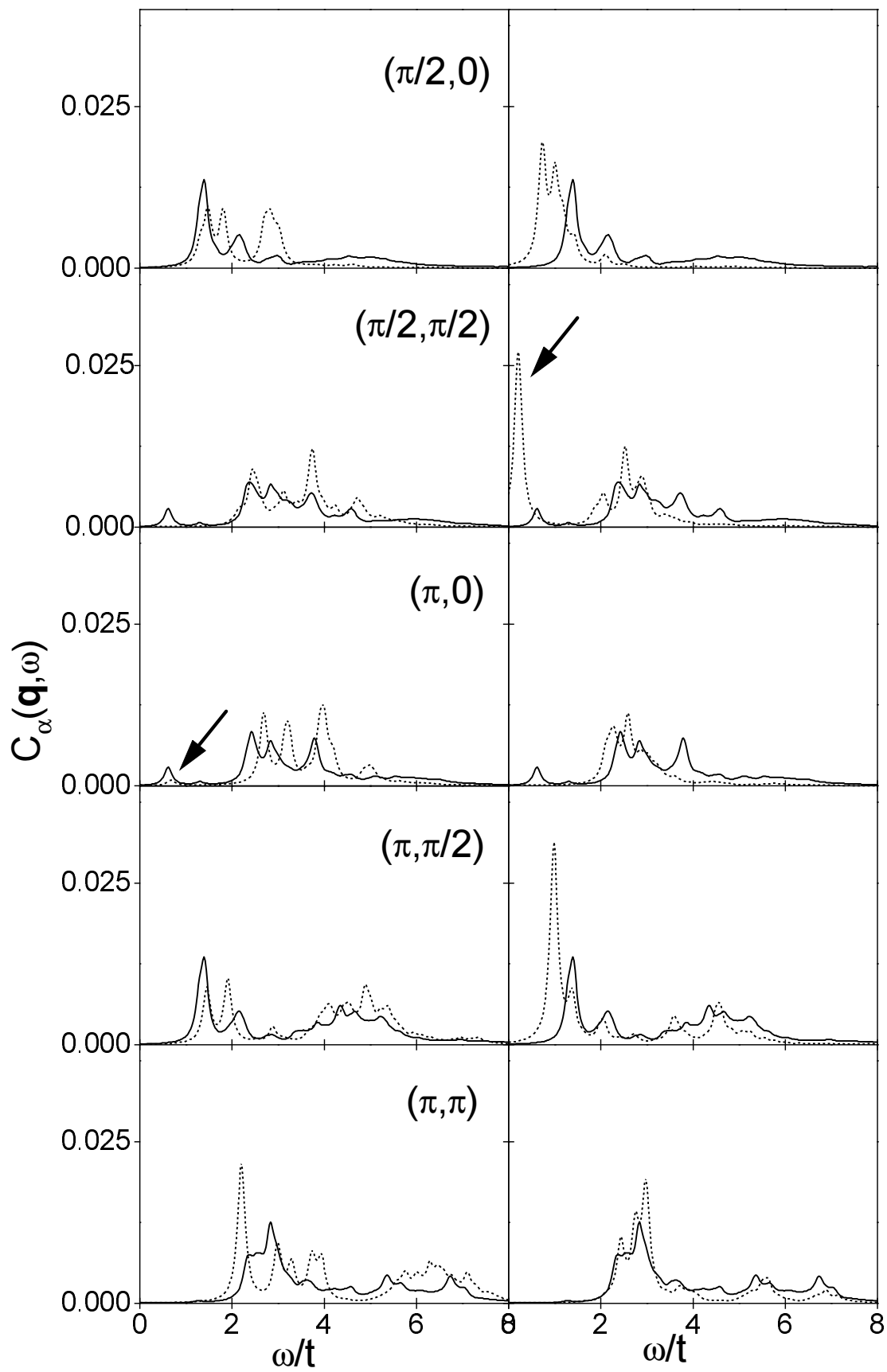


Fig. 3

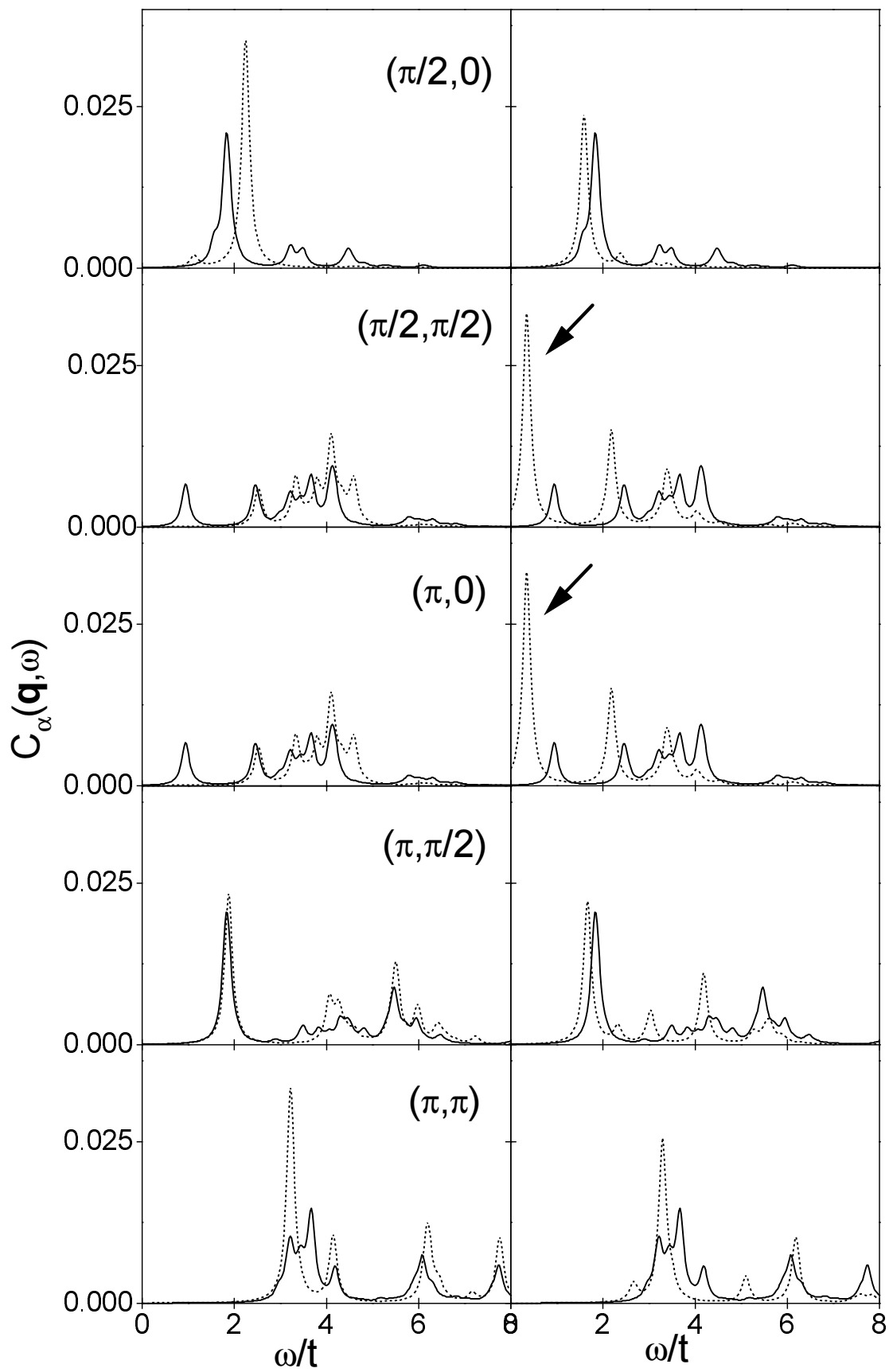


Fig. 4

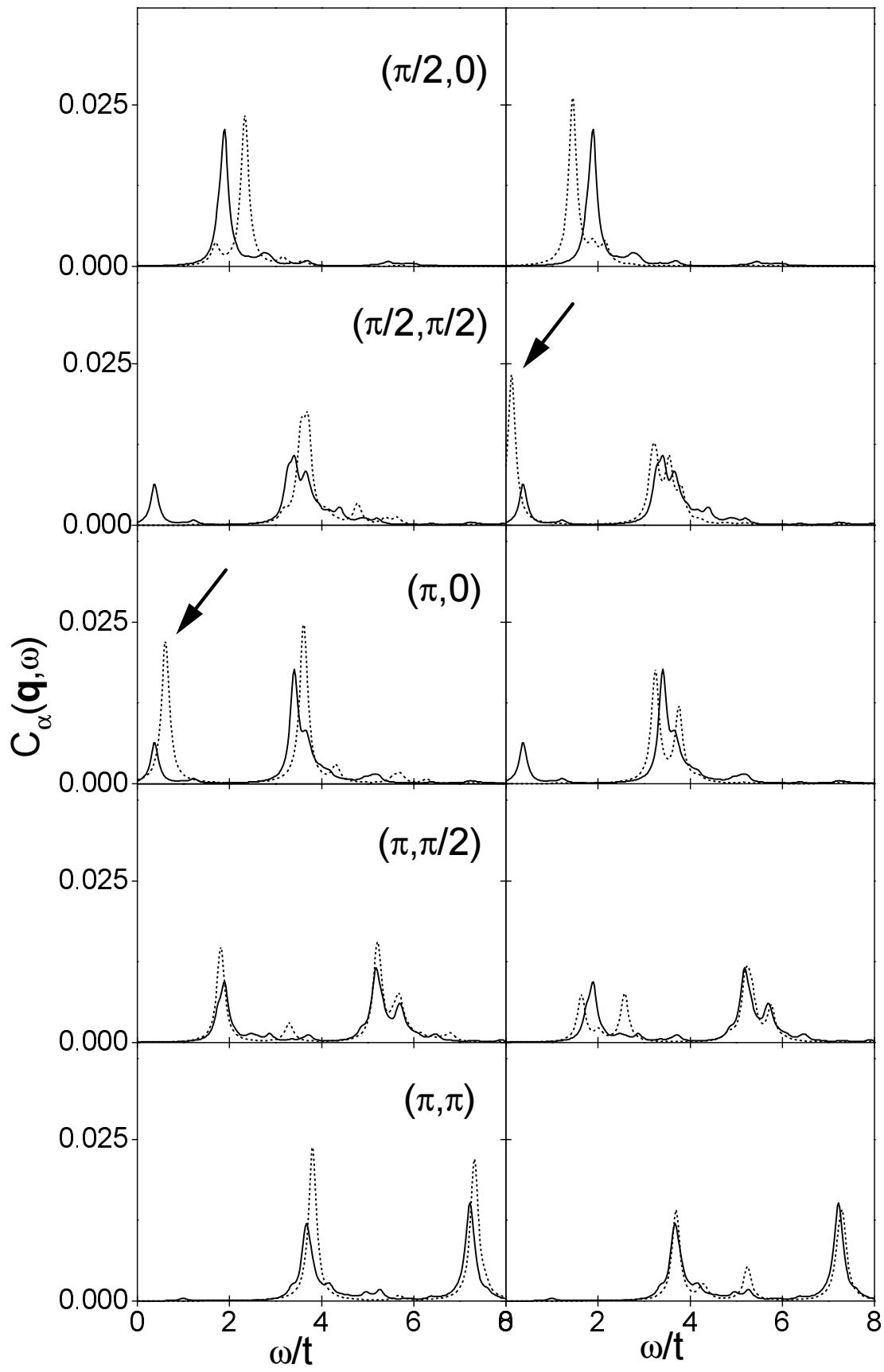
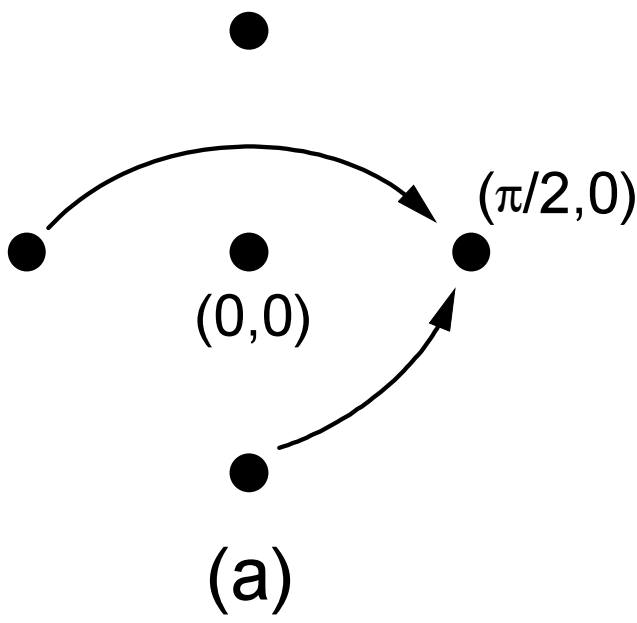
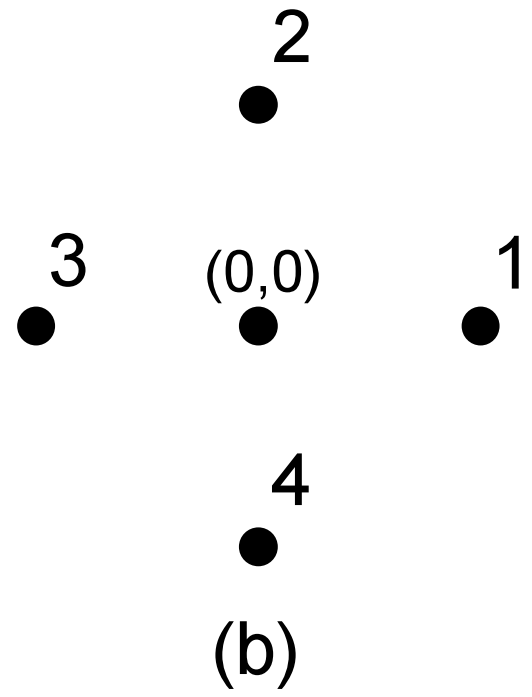


Fig. 5



(a)



(b)

Fig. 6

DCF, $\mathbf{k}=(\pi,0)$

+0.001 -0.016 +0.001 +0.008
○ ○ ○ ○

+0.035 +0.119 +0.035 -0.007
○ ● ○ ○

-0.190 -0.011 -0.190 +0.033
● ○ ● ○

+0.035 +0.119 +0.035 -0.007
○ ● ○ ○

SCF, $\mathbf{k}=(\pi/2,\pi/2)$

-0.005 +0.008 -0.001 0.003
○ ○ ○ ○

-0.001 +0.125 +0.021 -0.001
○ ● ○ ○

-0.141 -0.002 +0.125 +0.008
● ○ ● ○

+0.004 -0.141 -0.001 -0.005
○ ● ○ ○

Fig. 7

SCF, $\mathbf{k}=(\pi,0)$

+0.004 +0.010 +0.004 +0.004
○ ○ ○ ○

+0.004 -0.033 +0.004 +0.013
○ ● ○ ○

-0.014 0.000 -0.014 +0.033
● ○ ● ○

+0.004 -0.033 +0.004 +0.013
○ ● ○ ○

SCF, $\mathbf{k}=(\pi/2,\pi/2)$

+0.003 +0.004 +0.015 +0.004
○ ○ ○ ○

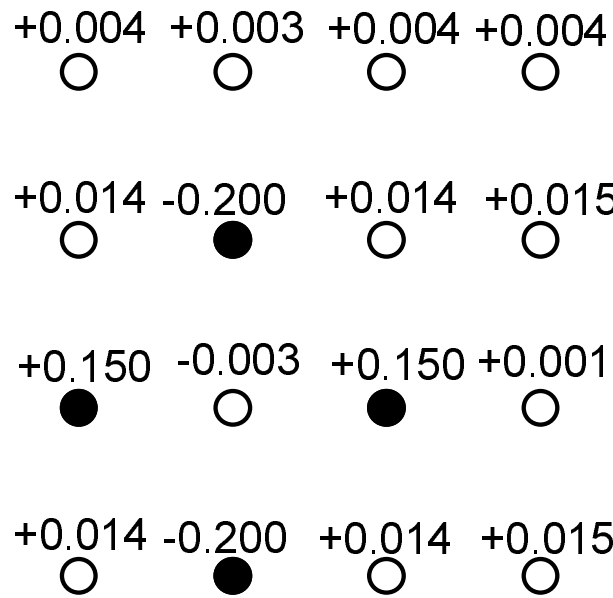
+0.009 +0.158 +0.020 +0.015
○ ● ○ ○

-0.207 0.000 +0.158 +0.004
● ○ ● ○

+0.013 -0.207 +0.009 +0.003
○ ● ○ ○

Fig. 8

DCF, $\mathbf{k}=(\pi,0)$



SCF, $\mathbf{k}=(\pi/2,\pi/2)$

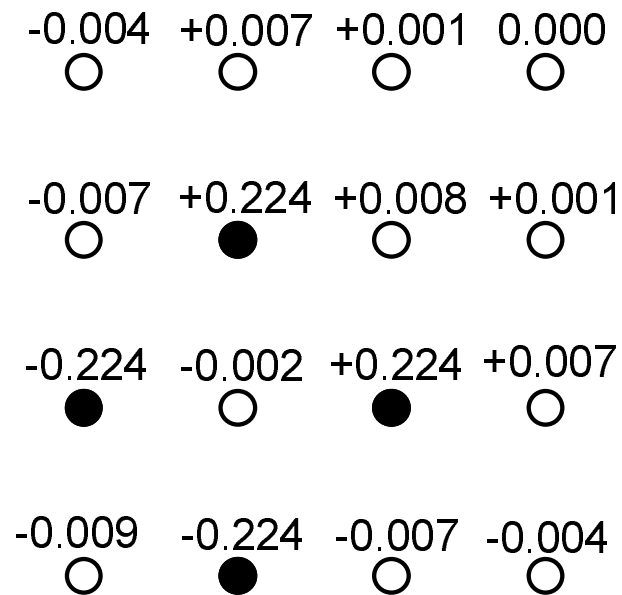


Fig. 9b

